Journal of Mining and Environment (JME) Vol. 17, No. 5, 2026, 1547-1565

Shahrood University of Technology

Journal of Mining and Environment (JME)

Journal homepage: www.jme.shahroodut.ac.ir

Iranian Society of Mining Engineering (IRSME)

Revalorization of Tailings in La Cienega (Peru) through Geochemical, Geostatistical modeling and Machine Learning Optimized by Metaheuristics

Marco Antonio Cotrina-Teatino[1*], Jairo Jhonatan Marquina-Araujo[1], Jose Nestor Mamani-Quispe[2], Jorge Chira-Fernandez[3], Cesar De la Cruz-Poma[3], and Solio Marino Arango-Retamozo[1]

1. Department of Mining Engineering, Faculty of Engineering, National University of Trujillo, Trujillo, Peru.
2. Faculty of Chemical Engineering, National University of the Altiplano of Puno, Puno, Peru.
3. Dirección de Recursos Minerales y Energéticos, INGEMMET, Lima, Peru

Article Info

Received 3 July 2025

Received in Revised form 7 October 2025

Accepted 9 December 2025

Published online 9 December 2025

DOI: 10.22044/jme.2025.16468.3212

Keywords

Mine tailings

Waste reprocessing

Geostatistics

Machine Learning

Metaheuristics

Abstract

The sustained increase in mining waste, particularly in the form of tailings, poses a significant environmental and economic challenge, especially in contexts where these deposits retain residual metal content. This study assessed the gold potential of Tailings Deposit I at La Cienega (Peru) by integrating geostatistical estimation and machine learning models optimized through metaheuristic algorithms. The methodology involved geochemical characterization, three-dimensional estimation using Ordinary Kriging (OK) as a geostatistical method, and prediction of gold grades through three models: XGBoost optimized with Particle Swarm Optimization (XGB+PSO), Support Vector Regression with Genetic Algorithm (SVR+GA), and Random Forest optimized using Ant Colony Optimization (RF+ACO). Estimates were validated using Leave-One-Out cross-validation and performance metrics including RMSE, MAE, Bias, and correlation coefficient (R). The RF+ACO model achieved an RMSE of 0.32 ppm, MAE of 0.24 ppm, Bias of 0.006, and an R value of 0.56. Average predicted grades ranged from 1.14 to 1.33 ppm, with estimated gold contents between 981.00 and 1,147.12 ounces, while OK yielded 1,028.77 ounces at an average grade of 1.19 ppm. These findings suggest that properly optimized machine learning models can provide reasonable estimates of metal content in tailings, particularly in settings characterized by high spatial heterogeneity and limited geological continuity.

1. Introduction

In recent decades, the intensification of mining activity driven by the growing demand for strategic metals has led to an unprecedented accumulation of industrial waste, with mine tailings representing one of the most voluminous and persistent byproducts [1, 2]. It is estimated that over 95% of extracted material is ultimately discarded as tailings, generating between five and seven billion tonnes annually worldwide [3, 4]. While the mining industry is essential for the energy transition and sustainable development, managing such waste presents large-scale technical, economic, and environmental challenges. Recent studies have emphasized that mine tailings, when analyzed using advanced predictive tools, provide valuable insights not only into resource recovery but also into long-term environmental behavior [5, 6].

In the case of gold mining, low processing efficiency often results in a significant fraction of the metal remaining trapped within sulfide mineral matrices such as pyrite, arsenopyrite, and pyrrhotite, which are subsequently discarded along with the tailings [7–9]. These residual accumulations not only represent an underutilized resource but also act as active sources of pollution when exposed to oxygen and water, generating acid mine drainage and releasing heavy metals [10, 11]. Additionally, abandoned tailings facilities pose physical risks due to structural instability, and their management frequently falls under public

Corresponding author: mcotrinat@unitru.edu.pe (M. Cotrina)

responsibility in the absence of clearly defined ownership [12, 13].

In response to this issue, the concept of circular mining has gained momentum, advocating for the revalorization of tailings as secondary sources of critical metals and industrial materials [14–19]. Recovery of elements such as Au, Cu, Co, In, and Ag has been reported from tailings in various geographic settings, using methods ranging from froth flotation and direct leaching to reuse in construction materials [20–24]. Furthermore, recent studies have shown that spatial analysis through geostatistics enables more precise quantification of the geochemical heterogeneity of such deposits, thereby supporting robust estimations of their economic value [10, 25–34].

In parallel, advances in data science have fostered the incorporation of machine learning (ML) algorithms to predict mineralogical and metallurgical properties, often outperforming classical approaches such as Ordinary Kriging (OK) [35–37]. Tools such as Random Forest, XGBoost, Support Vector Regression (SVR), and neural networks have been successfully applied to grade estimation in iron, copper, and gold deposits, demonstrating high coefficients of determination and superior adaptability to nonlinear relationships [38–40]. These capabilities have been enhanced through optimization techniques based on metaheuristics such as particle swarm optimization, genetic algorithms, or bee colony optimization, allowing for improved hyperparameter tuning and greater predictive accuracy in geologically complex environments [41–43]. In geological mapping and lithological classification, ensemble models such as StackingC and AdaBoost have also demonstrated high accuracy and generalizability [44–46]. These techniques are especially effective in complex terrains where traditional models struggle with non-linearity.

Machine learning models have also proven effective when integrated with geochemical fractal methods and deep learning-wavelet fusion techniques, offering novel strategies for geochemical anomaly detection and mineral prospectivity mapping [5, 47]. These hybrid frameworks highlight the potential of combining spatial statistics with AI in mineral exploration and critical element recovery [48].

In Peru, a country with strong economic dependence on mining and an extensive inventory of environmental liabilities, tailings deposits represent both a latent environmental hazard and an underexploited economic resource. The La Cienega deposit, located in the La Libertad region, has been documented in terms of its mineralogical characterization and socio-environmental risks [49–51], but lacks studies employing advanced predictive methods to quantify its reprocessing potential.

The novelty of this research lies in the integration of machine learning models optimized with metaheuristic algorithms to estimate the distribution and concentration of gold in an abandoned gold tailings deposit—an approach not previously applied in revalorization studies in Peru. This multidisciplinary methodology enhances estimation accuracy and offers a robust alternative to traditional techniques.

The general objective of this study is to assess the gold recovery potential of the La Cienega tailings deposit through the application of machine learning algorithms optimized with metaheuristics and spatial modeling techniques. This approach aims to support the development of more efficient and sustainable strategies for managing mining liabilities in similar contexts.

The structure of this article is as follows: Section 2 outlines the methodological framework; Section 3 presents and discusses the results; and Section 4 provides the general conclusions and proposes potential avenues for future research

2. Methodology

This study adopts a structured, sequential methodology that includes: (i) preprocessing and cleaning of geochemical data, (ii) spatial estimation using OK, (iii) predictive modeling with machine learning algorithms optimized via metaheuristic techniques, and (iv) validation using Leave-One-Out (LOO) cross-validation and statistical analysis, including Fisher's F-test. The overall research workflow is illustrated in Figure 1.

2.1. Geographical context and operational background of the La Cienega tailings deposit

The study area corresponds to the La Cienega tailings deposit, located in the Pataz District, Pataz Province, within the La Libertad region of northern Peru. The site lies at an average elevation of 2,960 meters above sea level, with approximate central coordinates of 215040 East and 9138860 North (WGS84 datum, UTM zone 18S) (see Figure 2). The facility consists of five individual tailings deposits, generated between 1990 and 2003, reflecting an operational legacy of more than three decades.

The mining concessions originally associated with this site were operated by Minera Pataz EPS. In the early 1990s, control of the operations was transferred to Marañon Gold Mining Company S.A., which inaugurated a gold processing plant in 1993 with a treatment capacity of 100 tons per day [50]. The metallurgical process involved cyanidation for gold leaching, followed by the Merrill-Crowe system, which comprises countercurrent washing and subsequent precipitation using zinc powder [52]. Operations ceased in 1996, leaving behind six mining environmental liabilities (PAM), including tailings and infrastructure from the processing plant.

Currently, Minera Poderosa S.A. holds the mining concessions formerly managed by Minera Pataz, and the La Cienega tailings deposit lies within its property. This site has been officially classified as "High Risk" by the Peruvian Ministry of Energy and Mines (MINEM) due to its potential environmental and geotechnical hazards.

According to a topographic survey conducted by [51], the total volume of the five deposits is estimated at approximately 31,000 m^3. Assuming an average dry density of 1.9 t/m^3, the total mass is estimated to be between 50,000 and 60,000 metric tons. From a granulometric standpoint, the tailings exhibit a relatively homogeneous fine-grained texture, predominantly silty clay and silty sand, with moisture content below 15%, suggesting a largely dry deposit condition.

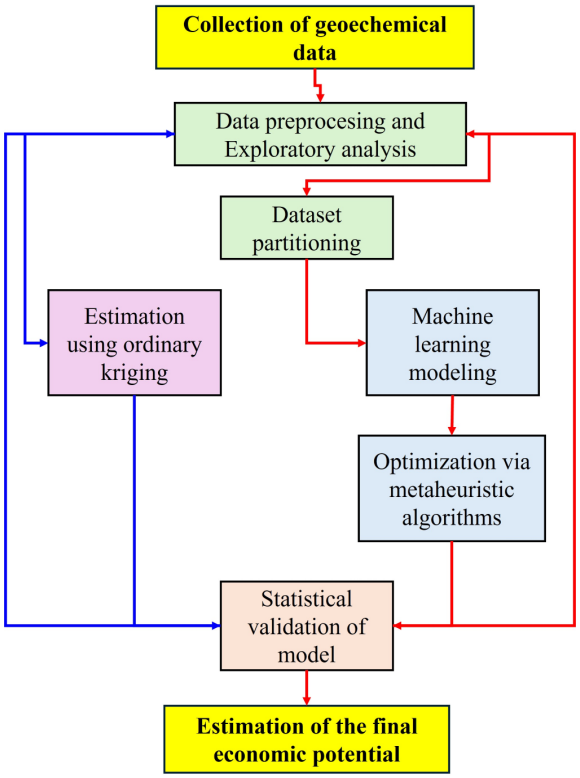

Figure 1. Flowchart of the methodological framework used for geochemical data modeling and validation

Figure 2. Geographical location of the La Cienega tailings facility in the Pataz District, La Libertad Region, northern Peru

2.2. Geological framework and mineralogy of the La Cienega deposit

The La Cienega area is part of the Pataz-Buldibuyo mining district, located in northern Peru, within an orogenic metallogenic belt that extends approximately 160 km in a northwest–southeast orientation. This gold-bearing zone is closely associated with the Pataz Batholith, a plutonic intrusion dated to approximately 330 million years (Ma), which lies in tectonic contact with a folded sequence of Paleozoic metasediments [53–55]. The gold mineralization, formed around ~313 Ma, is hosted in quartz-sulfide veins that trend predominantly northeast, affecting both the batholith and its sedimentary basement [55] (see Figure 3).

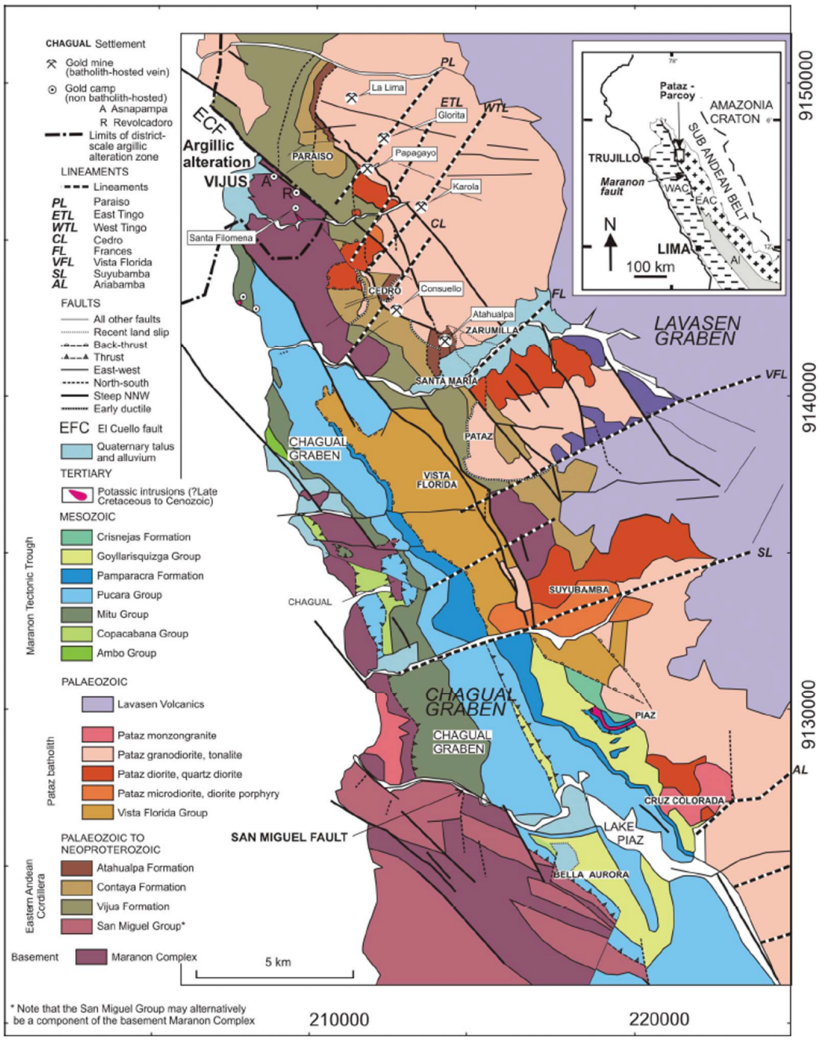

Figure 3. Regional geological map of the Pataz-Buldibuyo mining district, northern Peru

From a paragenetic perspective, Haeberlin et al. [53] identified three distinct mineralization stages: (1) an initial phase dominated by milky quartz, pyrite, arsenopyrite, and ankerite; (2) an intermediate stage with microgranular bluish-gray quartz, galena, sphalerite, chalcopyrite, antimony sulfosalts, native gold, and electrum; and (3) a late barren stage characterized by calcite-dolomite and quartz veinlets. The associated hydrothermal alteration of the host rocks is typified by sericite, chlorite, carbonates, and disseminated pyrite.

The veins in this region display relatively homogeneous mineralogy, predominantly composed of gangue minerals such as quartz, feldspar, hornblende, micas, clays, and carbonates. Ore minerals include native gold, electrum, and metallic sulfides of silver, lead, zinc, copper, antimony, iron, and arsenic [56, 57]. The metallogenic assemblage features elements such as Au, Ag, As, Fe, Pb, Zn, Cu, Sb, Bi, Te, and W, indicative of a complex hydrothermal system with multiple mineralizing episodes.

Several genetic models have been proposed to explain the origin of this mineralization. Ore, Voute, and Witt et al. [55, 58, 59] attribute gold formation to magmatic processes linked to the Pataz Batholith, within the conceptual framework of intrusion-related gold deposits. Specifically, Witt et al. [55] suggest a potential genetic connection between Au-Pb-Zn mineralization and volcanic activity related to the Lavasen-Esperanza event, which is preserved east of the batholith.

Recent mineralogical studies by Voute et al. [59] in quartz veins from the Santa María district, which includes the La Cienega area, enable comparison between the current mineralogical composition of the tailings and the original characteristics of the mined ore. According to Ore [58], the system features two distinct gold mineralization phases along with a vertical zoning of silver content. In this context, the San Lorenzo vein, located in the upper southern section of Santa María, is believed to have been the primary source of feed material during the early operational stages of La Cienega, explaining the elevated Ag and Sb concentrations observed in the older tailings.

Furthermore, Voute et al. [59] describe two paragenetic styles for gold: an early stage with refractory gold finely disseminated in arsenopyrite and arsenic-rich pyrite, and a later stage dominated by visible gold and electrum associated with base metal sulfides. The latter currently represents the primary target of ongoing mining operations in the Pataz region.

2.3. Sample collection, preparation, and processing

To capture both the lateral and vertical variability of the tailings deposit, a combined sampling strategy was adopted involving manual trench excavation and mechanized drilling using an AUGER system. This methodology allowed for a comprehensive approach to addressing the stratigraphic and spatial heterogeneity of the tailings body.

A principal trench (T1) was excavated in the western sector of Tailings Deposit I, reaching a depth of 8.61 meters. This trench provided a continuous sedimentary profile, enabling direct observation of the stratigraphic sequence from surface to base. Four macroscopic units were identified along the profile, differentiated by color, texture, and degree of alteration: (1) a weathered surface horizon with white to yellowish tones; (2) unoxidized tailings layers, predominantly dark gray in color; (3) transitional layers exhibiting partial oxidation; and (4) heterogeneous strata with variable lithologies over short vertical intervals.

In addition, six AUGER drillholes were completed to an average depth of 4.0 meters and strategically distributed across Deposit I. Sampling points LC1, LC2, and LC3 were located in the western, central, and eastern sectors, respectively, to assess horizontal variability. Points LC4, LC5, and LC6 were aligned parallel to the main trench and positioned at different elevations along the western flank of the deposit, aiming to evaluate lateral continuity and verify sampling consistency (see Figure 4).

The AUGER drill system used was a portable, manually operated device suitable for remote or difficult-access areas. Drilling was carried out using 1-meter-long auger rods with a diameter of 8 cm. Samples were collected at regular 25 cm intervals, allowing for up to eight subsamples per borehole. Each subsample was stored in sealed plastic cylinders to preserve original moisture and prevent post-sampling alteration. A total of 109 geochemical samples were collected for gold content determination, distributed across trench T1 and the six drillholes.

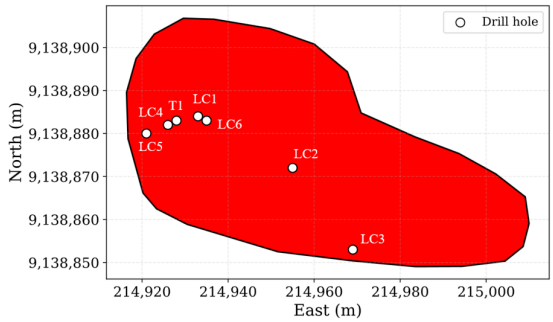

Figure 4. Geometry of tailings deposit I at La Cienega, showing the spatial distribution of trench and AUGER drillhole sampling locations

2.4. Geostatistical modeling of gold content

A 3D geostatistical model was developed to estimate the gold distribution within Tailings Deposit I at La Cienega, based on the geochemical data collected in the field. A uniform cubic block grid of 1 m × 1 m × 1 m was defined, fitted to the geometry of the deposit and linked to a topographic surface obtained via a total station survey. A reference elevation of 2950 masl was adopted, and a constant dry density of 1.90 t/m^3 was assumed for total mass calculations.

Prior to interpolation, a univariate analysis of Au concentrations was performed, followed by the construction of omnidirectional experimental variograms. These were fitted with theoretical

models (spherical, exponential, or Gaussian), defining nugget, sill, and range parameters [60, 61].

Gold grade estimation for each block was performed using ordinary kriging (OK), a technique that assigns optimal weights based on the spatial correlation structure described by the fitted variogram. The general interpolation formula is:

$$\hat{Z}(x_0) = \sum_{i=1}^{n} \lambda_i Z(x_i) \quad (1)$$

where, $\hat{Z}(x_0)$ is the estimated value at location x_0, $Z(x_i)$ is the measured value at location x_i, and λ_i is the weight assigned to each sample point.

Ordinary kriging was selected over more complex approaches such as cokriging due to the absence of well-correlated and georeferenced secondary variables. Moreover, OK provides a robust solution and is less prone to overfitting in univariate models [38, 62–64]. The modeling was implemented in Python 3.11.7 using the Jupyter Notebook environment, with the scikit-gstat library for variogram fitting and pykrige for kriging interpolation.

2.5. Predictive modeling with machine learning algorithms optimized via metaheuristics

To enhance the accuracy of gold grade estimations based on geochemical data, machine learning (ML) algorithms were implemented in combination with bioinspired optimization techniques. These hybrid approaches enable automated tuning of model hyperparameters, significantly improving predictive performance in contexts characterized by nonlinear relationships and high spatial variability. The models employed in this study were: (1) Extreme Gradient Boosting optimized with Particle Swarm Optimization (XGB+PSO); (2) Support Vector Regression optimized with a Genetic Algorithm (SVR+GA); and (3) Random Forest optimized using Ant Colony Optimization (RF+ACO).

The selection of specific metaheuristic algorithms for each machine learning model was based on previous benchmarking studies in mining-related prediction tasks and the known compatibility between certain optimizers and model structures. PSO has demonstrated strong performance in tree-based boosting models such as XGBoost, especially in high-dimensional search spaces [65, 66]. GA has been widely used for tuning kernel-based models like SVR due to their robustness in navigating complex, nonlinear parameter landscapes [67]. ACO has shown promising results in ensemble-based algorithms such as Random Forest by efficiently exploring discrete parameter combinations [68]. Although applying all optimizers to all models could provide further comparative insights, the focus of this study was to evaluate the feasibility and complementarity of selected hybrid combinations rather than exhaustively test all permutations.

XGBoost is a decision tree-based boosting algorithm that builds sequential models by minimizing a regularized objective function [69–72]. Its general formulation is expressed as:

$$\hat{y}_i = \sum_{k=1}^{K} f_k(x_i), \quad f_k \in F \quad (2)$$

where $\hat{y}_i$ is the predicted value for sample i, f_k is the regression tree at iteration k, F is the space of CART regression trees.

PSO was employed to tune key hyperparameters such as the number of trees K, leaning rate η, maximum tree depth, and the regularization parameter λ. PSO iteratively updates a population of candidate solutions ("particles") based on both individual and global best experiences to converge on optimal configurations [73, 74].

SVR seeks to construct a non-linear regression function that minimizes model complexity and prediction error within an acceptable margin ε [75]. The standard formulation is:

$$f(x) = \sum_{i=1}^{n} (\alpha_i - \alpha_i^*) K(x_i, x) + b \quad (3)$$

where $K(x_i, x)$ is the kernel function is typically a radial basis function (RBF), $\alpha_i - \alpha_i^*$ are Lagrange multiplier, and b is the model bias.

GA were used to optimize parameters such as the penalty term C, kernel width γ and ε, using standard genetic operators crossover, mutation, and selection applied to encoded populations of candidate solutions [76].

RF is an ensemble learning method based on aggregating multiple decision trees built from bootstrap samples and random feature subsets [77]. Predictions are generated through:

$$\hat{y} = \frac{1}{T} \sum_{t=1}^{T} h_{t(x)} \quad (4)$$

where $h_{t(x)}$ is the prediction of the $t - th$ tree and T is the total number of trees. To enhance model performance, ACO was applied to tune hyperparameters such as the number of trees T,

maximum features per split, and maximum tree depth. ACO simulates the pheromone-guided foraging behavior of ants to converge on high-performing parameter configurations [78].

All models were implemented in Python 3.11.7. The libraries used included XGBoost, scikit-learn, and DEAP for SVR+GA, while custom implementations of PSO and ACO were developed using pyswarms and ACOpy, respectively.

2.6. Validation of predictive models

Model validation was performed using the Leave-One-Out Cross-Validation (LOO) method, a robust approach in which each sample in the dataset is iteratively excluded from the training set and independently predicted [79]. This technique enables rigorous evaluation of the model's generalization capability, as each iteration involves training on $n-1$ observations and testing on the excluded sample.

The prediction error for each observation was computed as:

$$\varepsilon_i = Z(x_i) - \hat{Z}_{-i}(x_i) \quad (5)$$

where $Z(x_i)$ is the actual gold concentration at location x_i. $\hat{Z}_{-i}(x_i)$ is the estimated value excluding point x_i from training, and ε_i represents the residual error for that prediction. To assess the overall performance of each model, the following statistical metrics were calculated [80].

MAE (Mean Absolute Error): the average of the absolute differences between predicted and observed values. RMSE (Root Mean Square Error): the square root of the mean squared error, which emphasizes larger errors. Bias: the average residual error, used to detect systematic over- or underestimation. R (Pearson Correlation Coefficient): the linear correlation between observed and predicted values [37, 81, 82].

3. Results

As shown in Table 1, the maximum concentrations of elements such as As, Pb, Sb, and Cu were significantly higher than their respective means prior to data preprocessing, indicating the presence of influential outliers. Following the application of a capping procedure, a systematic reduction in standard deviation was observed, particularly for critical elements such as Cu (from 68.41 to 65.83 ppm) and Fe (from 1.43% to 1.39%). This suggests a successful reduction in data dispersion without altering the central tendency. This preprocessing step was essential to minimize statistical bias and improve the robustness of the predictive models used in subsequent stages.

Table 1. Descriptive statistics of geochemical variables before and after data preprocessing

	Unit	Statistics before processing				Statistics after processing			
		Mean	Stdev	Min	Max	Mean	Stdev	Min	Max
As	ppm	8173.60	1995.42	4245	15359	8175.42	1951.71	4864.74	14861.36
Cd	ppm	42.00	20.70	13.6	90.4	41.89	20.46	13.67	83.27
Pb	ppm	3777.06	2464.29	378	13733	3771.29	2396.27	953.52	12770.72
Zn	ppm	1453.90	711.72	479	3727	1451.62	704.11	485.60	3567.94
Cr	ppm	206.61	77.57	120	545	205.22	71.69	125.28	446.66
Mn	ppm	1577.46	397.67	295	2661	1576.67	392.33	331.30	2571.24
Co	ppm	19.97	5.13	8.7	47.1	19.85	4.34	10.68	36.74
Ni	ppm	41.17	10.50	17	66.4	41.23	10.30	21.88	65.21
V	ppm	110.34	17.72	76	172	110.24	16.93	81.94	158.80
Sb	ppm	38.76	40.71	9.9	197	38.74	40.50	11.42	193.70
Ti	ppm	2323.08	692.25	1525	5075	2311.48	649.70	1540.84	4282.34
Sc	ppm	12.33	3.65	8.3	31	12.21	3.12	8.56	23.08
Au	ppm	1.42	0.38	0.1	2.56	1.42	0.36	0.85	2.41
Cu	ppm	150.85	68.41	80.6	431	150.19	65.83	80.73	386.78
Fe	%	7.11	1.43	4.7	13	7.10	1.39	4.83	12.34
Al	%	4.26	0.82	3.17	7.61	4.24	0.76	3.26	6.43
Ca	%	2.46	0.50	1.5	4.40	2.46	0.47	1.63	3.87
Mg	%	1.24	0.34	0.72	2.91	1.23	0.30	0.75	2.40
Ba	ppm	193.16	53.88	117	400	192.34	50.87	118.98	342.58
K	%	1.64	0.34	0.7	2.80	1.64	0.31	1.01	2.49
Na	%	0.40	0.29	0.13	2.23	0.39	0.22	0.13	1.49
Sr	ppm	63.43	19.03	34.8	123	63.48	18.92	38.17	122.34

For gold, the initially strong right-skewed distribution was slightly corrected, resulting in a more compact and symmetric shape. This adjustment improves the statistical quality of the dataset and reduces the risk of overfitting in machine learning models, especially those

sensitive to outliers (SVR). Importantly, the capping procedure preserved the overall structure of the data, maintaining the essential geochemical variability required for subsequent analysis (see Figure 5).

Figure 6 reveals key linear relationships relevant to predictive modeling. Specifically, gold shows strong positive correlations with copper, iron, arsenic, and antimony, supporting their selection as independent variables in the estimation models. These associations align with typical mineralogical patterns, such as gold hosted in iron sulfides or arsenic-bearing phases. Spatial coordinates (X, Y, Z) were also incorporated into the modeling process, as they help capture local concentration gradients across the deposit. The absence of strong negative correlations suggests no antagonistic geochemical behaviors, facilitating the integration of multiple variables in machine learning algorithms.

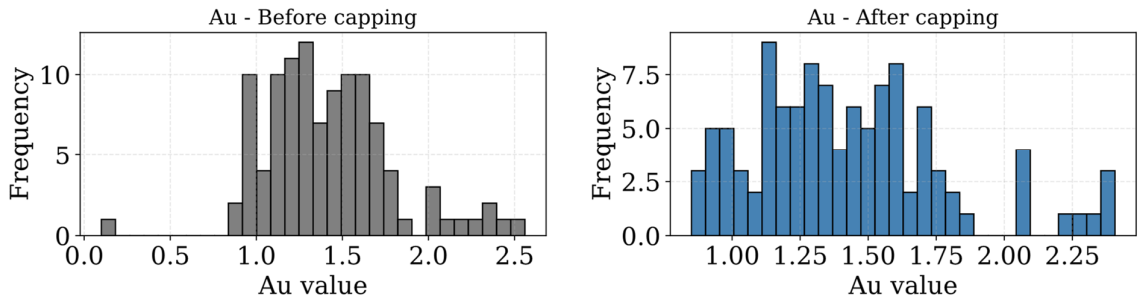

Figure 5. Frequency histograms of Au concentrations before (left) and after (right) capping of extreme values

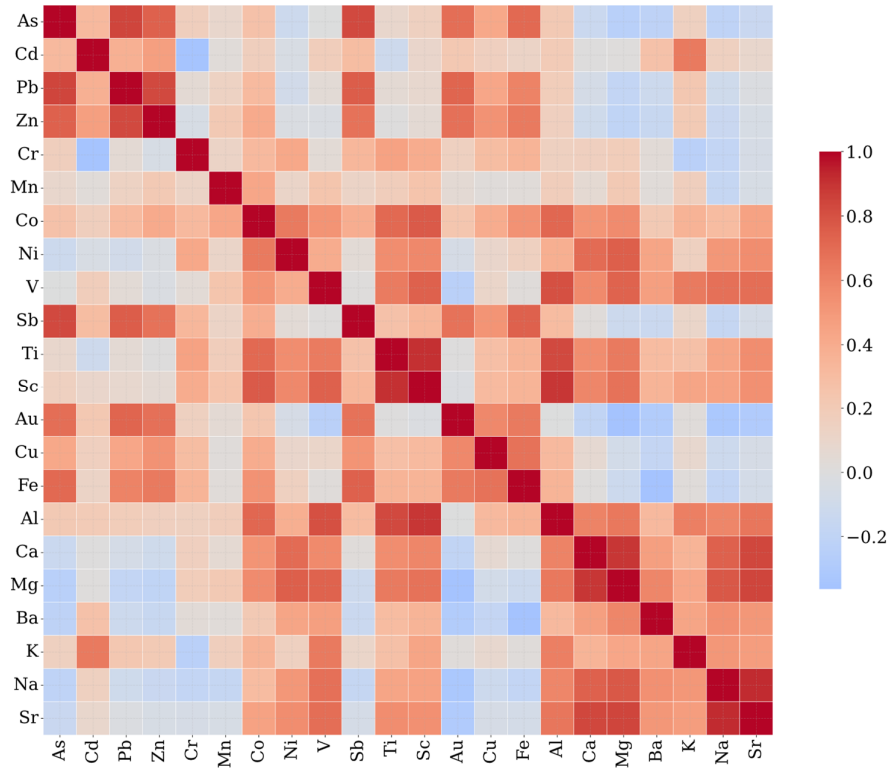

Figure 6. Pearson correlation matrix of 22 geochemical variables from tailings deposits I at La Cienega

Following the correlation analysis, the spatial continuity of the main geochemical variables was evaluated through variogram modeling. Figure 7 presents the omnidirectional experimental variograms and fitted spherical models, along with the anisotropy ellipses derived from directional variogram analysis for Au, Cu, Fe, As, and Sb. These five elements were selected based on their strong correlations with Au and their known mineralogical associations in tailings.

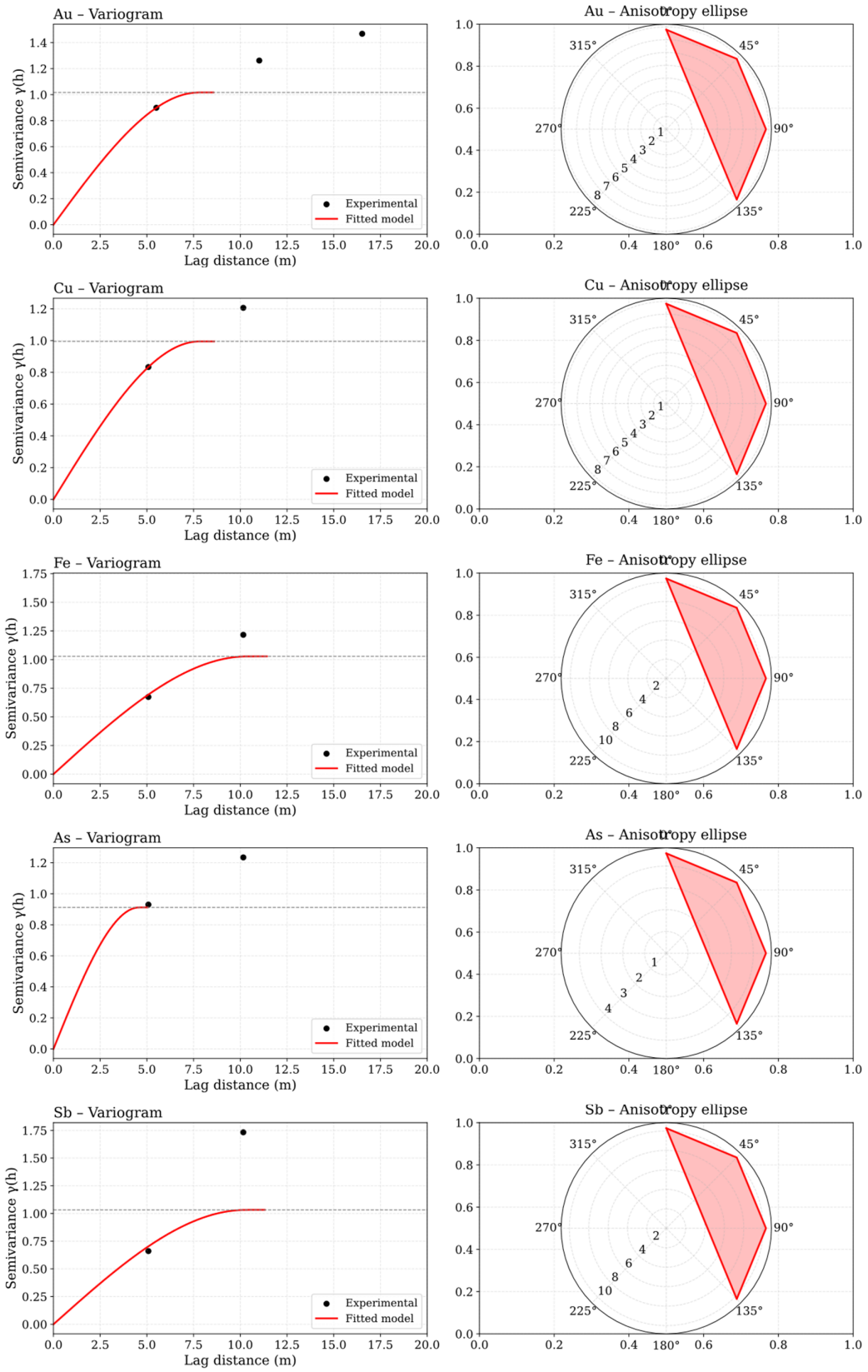

Figure 7. Experimental variograms and anisotropy ellipses for Au and key associated elements (Cu, Fe, As, Sb) in Tailing Deposit I

Optimal hyperparameters were selected using bioinspired global search algorithms to maximize the predictive performance of each model. For XGBoost+PSO, 15 particles and 5 dimensions were used within a bounded parameter space. For SVR+GA, a population of 20 individuals across 30 generations was employed, incorporating penalties for invalid hyperparameter combinations. In the case of RF+ACO, combinations of n_estimators ranging from 50 to 300 and max_depth between 3 and 20 were explored over 10 iterations with 10 ants (see Table 2).

Table 2. Optimal hyperparameters for machine learning models tuned with metaheuristic algorithms

Model	Hyperparameter	Value
XGB+PSO	N estimators	140
	Max depth	14
	Learning rate	0.283
	Subsample	0.72
	Colsample bytree	0.52
SVR+GA	C	111.25
	Epsilon	0.07
	Gamma	1.26
RF+ACO	N estimators	295
	Max Depth	3

The Ordinary Kriging model produced a smooth interpolated surface, with maximum concentrations around 2.0 ppm in the western sector and a gradual decline to approximately 1.0 ppm toward the east. In contrast, the machine learning models optimized via metaheuristics demonstrated an enhanced ability to capture local high-grade zones. The XGB+PSO model predicted a compact mineralized core with values near 2.2 ppm, aligning with high-concentration areas confirmed by drilling. This performance is attributed to the model's deep tree structure and learning rate, which allow it to capture nonlinear interactions among variables (see Figure 8).

The SVR+GA model produced a similar but more focused high-grade zone, with peak values around 1.8 ppm and sharper spatial boundaries. This behavior is consistent with SVR's ability to model sharp margins using kernel functions. Conversely, the RF+ACO model resulted in a more spatially uniform and conservative estimation, with maximum concentrations near 1.9 ppm and greater smoothing. This outcome is characteristic of the ensemble averaging behavior in Random Forest and the relatively shallow tree depth (max depth = 3) selected during optimization.

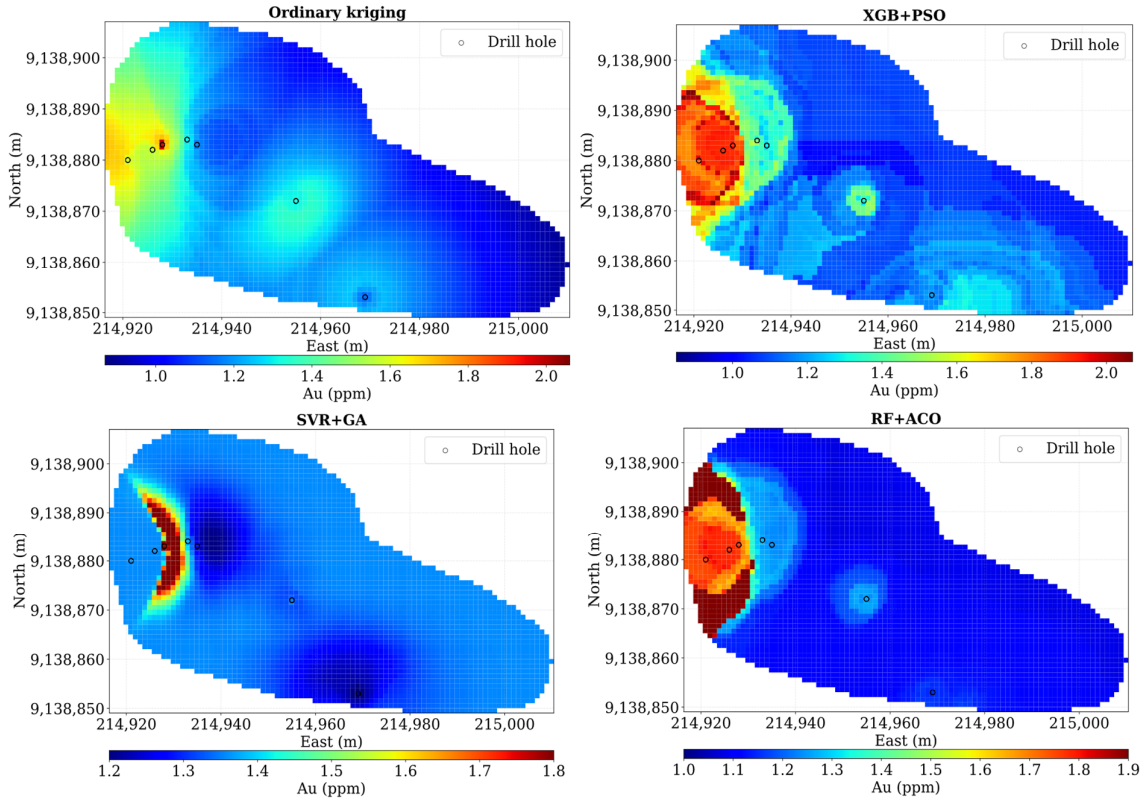

Figure 8. Spatial estimation maps of gold content in Tailings Deposit I at La Cienega generated using Ordinary Kriging and three machine learning models optimized with metaheuristics

The performance of the estimation models was assessed using Leave-One-Out cross-validation (LOO), with the results illustrated in Figure 9 and presented in Table 3. The geostatistical model based on OK exhibited the highest accuracy overall, with the lowest RMSE (0.24 ppm), MAE (0.18 ppm), and the strongest linear correlation (R = 0.74). However, it also showed a tendency to smooth high-grade anomalies, underestimating local maxima. In contrast, the RF+ACO model achieved the most balanced performance among the machine learning models (RMSE = 0.32 ppm, MAE = 0.24 ppm, R = 0.56), suggesting its robustness in capturing nonlinear patterns. These results highlight the complementary nature of both geostatistical and machine learning approaches in tailings modeling.

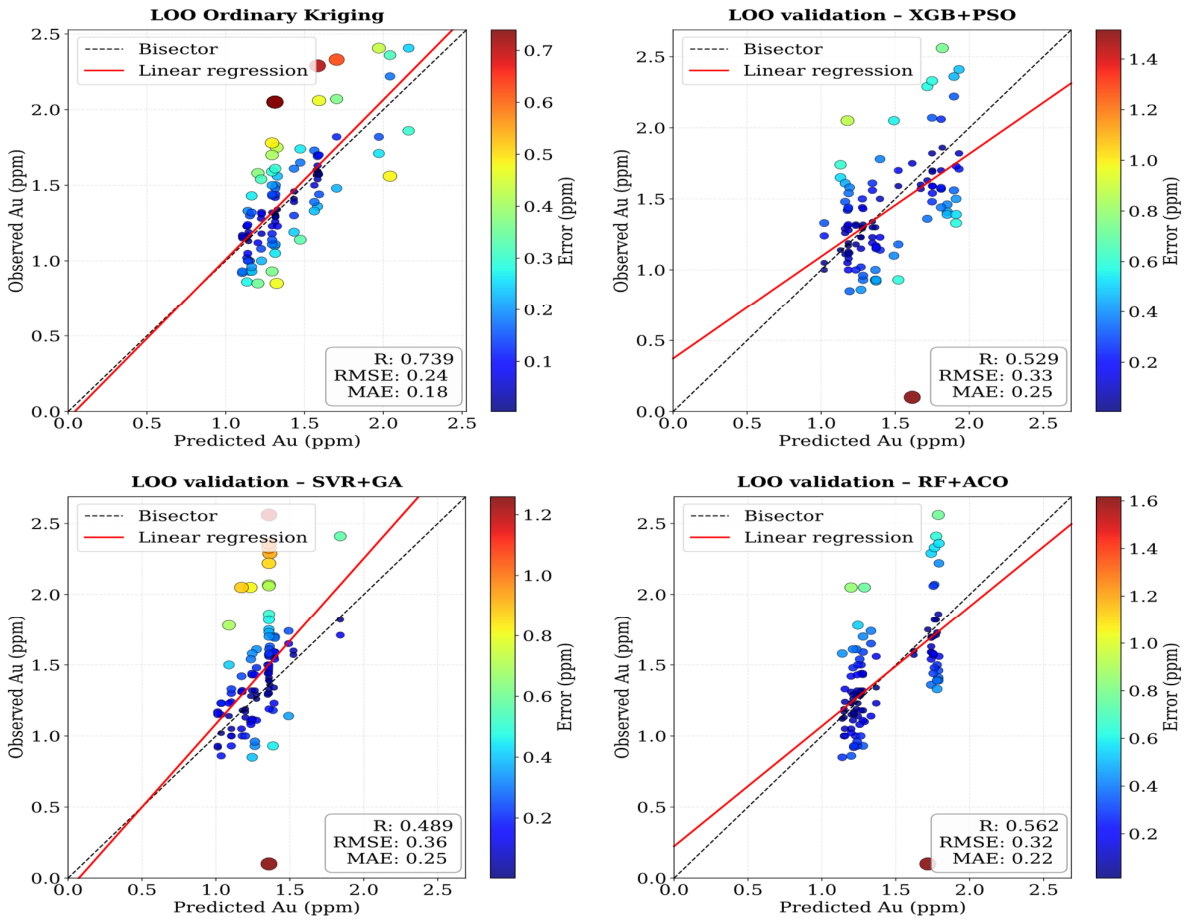

Figure 9. LOO validation of gold grade estimates using Ordinary Kriging and machine learning models optimized with metaheuristics

Table 3. Validation metrics for gold grade estimation using machine learning models

Model	MAE	Bias (mean error)	RMSE	R
OK	0.18	0.03	0.24	0.74
XGB+PSO	0.25	-0.03	0.33	0.53
SVR+GA	0.25	0.13	0.36	0.49
RF+ACO	0.24	0.006	0.32	0.56

To quantify the effect of the metaheuristic optimization, the relative differences (Δ) between unoptimized and optimized models were calculated for all performance metrics (Table 4). The results demonstrate that optimization improved predictive performance in all cases, especially for Random Forest and XGBoost. The RF+ACO model showed an 8.6% reduction in RMSE and a 12% increase in R, while XGB+PSO achieved a 13.8% reduction in MAE and a 12.8% gain in correlation. Although the improvements appear moderate in magnitude, they are significant considering the strong spatial

heterogeneity and small sample size characteristic of the dataset. These findings confirm that the optimization process effectively refined the hyperparameter space, enhancing model robustness and generalization under geologically complex conditions.

Table 4. Comparison of model performance before and after metaheuristic optimization

Model	Optimization method	ΔMAE (%)	ΔBias (%)	ΔRMSE (%)	ΔR (%)
XGB	PSO	-13.8	-234.6	-5.7	+12.8
SVR	GA	-16.7	+1400.0	0.0	+4.3
RF	ACO	-14.3	-33.3	-8.6	+12.0

Negative Δ values indicate error reduction, positive ΔR represents improvement in correlation.

Figure 10 presents spatial maps of prediction error (defined as predicted minus observed values) for the three machine learning models. The XGB+PSO and RF+ACO models tend to overestimate gold concentrations along the periphery of the mineralized zone, whereas the SVR+GA model exhibits a systematic underestimation in the central area. These spatial patterns are further supported by the error distribution plots in Figure 11, where the RF+ACO model displays a centered and symmetric distribution around zero, indicating minimal bias. In contrast, the XGB+PSO model shows a slightly negative skew, while SVR+GA exhibits a slight positive bias.

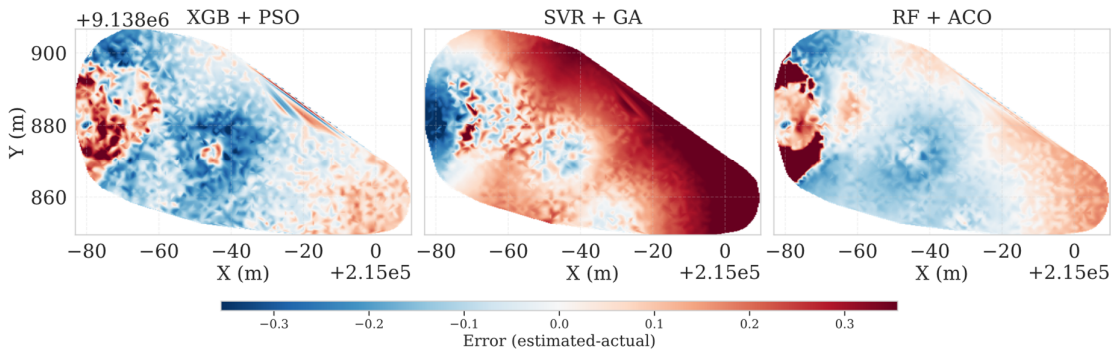

Figure 10. Spatial distribution of prediction errors (predicted – observed) for gold grade using machine learning models optimized with metaheuristics in Tailings Deposit I, La Cienega

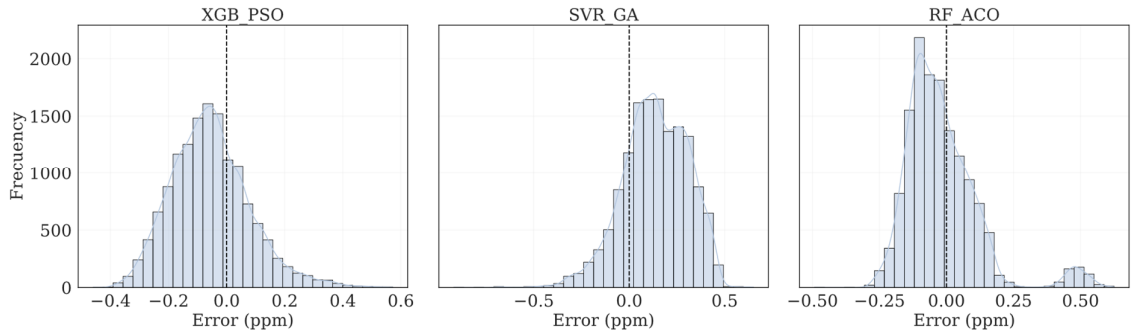

Figure 11. Error distribution plots for gold grade predictions from machine learning models optimized with metaheuristic algorithms

In addition, the F-test was applied to compare the error variance of the OK model with those of the machine learning models (Table 5). In all cases, statistically significant differences were found (p-value < 0.05), indicating that the ML models exhibit error structures distinct from OK. Although the RF+ACO model approached a similar variance level, the difference remained statistically significant. This confirms that AI-based algorithms offer a differentiated estimation pattern with potential to capture nonlinearities overlooked by classical linear methods.

Table 5. Fisher's F-test for variance comparison between OK and ML models optimized with metaheuristics

Model	Variance	F	p-value	Result
OK	0.026	1.434	2.22×10^{-16}	Significant difference
XGB+PSO	0.018			
OK	0.026	1.108	1.21×10^{-9}	Significant difference
SVR+GA	0.029			
OK	0.026	1.312	2.22×10^{-16}	Significant difference
OK	0.026			

The geostatistical estimation using OK reported an average grade of 1.19 ppm and a total tonnage of 26,843.20 metric tons, corresponding to 1,028.77 ounces of gold. This value is adopted as a reference due to its methodological validation and widespread use in mineral resource estimation studies. In comparison, machine learning models optimized with metaheuristics produced variable outcomes. The SVR+GA model yielded the highest average grade at 1.33 ppm, estimating a total of 1,147.12 ounces of gold, even surpassing the OK estimate. However, this result should be interpreted with caution, as the higher grade could reflect lower sensitivity to spatial bias, as evidenced in previous validation results. The XGB+PSO model produced the most conservative estimate, with an average grade of 1.14 ppm and an estimated content of 981.00 ounces, while the RF+ACO model, with an average grade of 1.18 ppm, predicted 1,014.02 ounces of gold. This result showed strong consistency with the OK estimates, both in magnitude and spatial distribution (see Table 6).

Table 6. Estimated economic potential of gold in Tailings Deposit I of La Cienega

Model	Average grade (ppm)	Total material (tons)	Gold (ounces)
OK	1.19	26843.20	1028.77
XGB+PSO	1.14		981.00
SVR+GA	1.33		1147.12
RF+ACO	1.18		1014.02

Figure 12 illustrates the inverse relationship between average gold grade and the volume of recoverable material under varying cut-off values. In this plot, the SVR+GA and RF+ACO models demonstrate more stable behavior across intermediate cut-off ranges (1.3–1.6 ppm), while the OK and XGB+PSO models exhibit greater sensitivity to threshold changes. Notably, the RF+ACO model produces a grade-tonnage curve that more closely resembles the expected behavior of real mineral deposits, indicating a more balanced trade-off between accuracy and robustness in the presence of spatial variability. These findings suggest that, although machine learning models optimized with metaheuristics are not intended to replace traditional geostatistical estimations, they serve as valuable complementary tools, particularly in complex settings like tailings deposits, where spatial continuity is often difficult to capture using classical techniques. Within the scope of this study, the RF+ACO model emerged as the most reliable approach in terms of estimation accuracy and consistency in assessing economic potential.

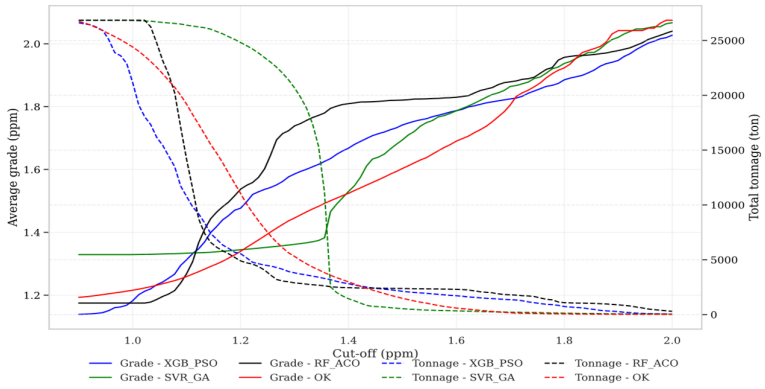

Figure 12. Grade-tonnage curves for gold estimation using geostatistical and machine learning models in Tailings Deposit I at La Cienega

The results obtained in this study provide significant evidence of the potential for applying hybrid approaches that integrate geostatistical modeling and machine learning to estimate metal content in gold tailings deposits, such as the case of La Cienega. Traditional techniques like OK have long been validated in the mining industry due to their theoretical robustness and capacity to account for spatial continuity [62, 63]. However, in tailings contexts where original stratigraphy is often disrupted and mineral distribution patterns exhibit high heterogeneity, conventional techniques may fail to capture the nonlinear relationships between predictor variables and metal concentrations.

The use of machine learning algorithms optimized with metaheuristics proved to be a viable alternative. In particular, the RF+ACO model demonstrated outstanding performance, both in Leave-One-Out cross-validation (with R = 0.56 and RMSE = 0.32 ppm) and in estimating total gold content (1,014.02 oz), closely aligning with the OK model (1,028.77 oz). This consistency is especially noteworthy given that machine learning models, unlike kriging, do not require assumptions of stationarity or variogram construction, offering an operational advantage when working with noisy data, such as those commonly encountered in tailings [38, 80].

Although the SVR+GA model produced higher estimates (1,147.12 oz), it exhibited larger error margins (RMSE = 0.36 ppm) and a positive bias in cross-validation, likely due to overfitting to localized structures in the training dataset. This phenomenon has been previously noted in studies on non-parametric regression applied to soil geochemistry [37, 60], supporting the importance of evaluating spatial error stability, an aspect addressed through the error maps and distributions presented in this study.

Another relevant finding was the strong correlation observed between gold and elements such as arsenic, antimony, iron, and copper, which aligns with the mineralogical characterizations reported by Witt et al. [55] and Voute et al. [59] for the Pataz region. These associations suggest that multielement geochemistry can serve as a reliable proxy for identifying zones of higher metal potential, even in the absence of a dense drilling grid. Additionally, processed histograms showed clear improvement in the distribution of key variables following capping, which reduced skewness and the influence of outliers that commonly distort predictive models.

From an economic perspective, the estimated content of over 1,000 ounces of gold in Deposit I represents a significant volume, especially considering that the material was historically discarded. This finding reinforces the feasibility of tailings reprocessing strategies as a means of recovering precious metals and extending the operational life of mining projects, consistent with the proposals of Mpinga et al. [52] and Ramadhan et al. [61]. Moreover, this approach offers an environmental advantage by mitigating high-risk mining liabilities such as La Cienega, which is officially classified as high impact by the Peruvian Ministry of Energy and Mines (MINEM). Operationally, the use of models like RF+ACO offers a practical tool for identifying high-grade zones within a tailings body, which can inform selective sampling or recovery campaigns. While it does not replace kriging for regulatory compliance in resource reporting, it can complement preliminary analysis and support decision-making in remediation or economic revaluation projects.

4. Conclusions

The results of this research demonstrate that integrating geostatistical techniques with machine learning models optimized through metaheuristic algorithms constitutes a methodologically robust framework for estimating gold content in heterogeneous tailings deposits such as Deposit I at La Cienega. The OK model provided a reference estimate of 1,028.77 ounces of gold at an average grade of 1.19 ppm, achieving the highest accuracy metrics (RMSE = 0.24 ppm, MAE = 0.18 ppm, R = 0.74). This confirms its effectiveness in modeling spatially continuous phenomena and its reliability as a baseline estimator in mineral resource assessments.

Among the machine learning approaches, RF+ACO demonstrated the most consistent performance, producing an estimate of 1,014.02 ounces with MAE = 0.24 ppm, RMSE = 0.32 ppm, and R = 0.56. Although its accuracy was slightly lower than that of OK, the RF+ACO model provided more stable results under complex spatial variability, highlighting its robustness and reduced bias. In contrast, the SVR+GA and XGB+PSO models showed higher errors and moderate sensitivity to local anomalies, confirming that ensemble-based models tend to outperform kernel- or boosting-based algorithms in irregular datasets. Overall, these results underscore the complementary nature of geostatistical and machine learning approaches: while OK remains the preferred standard for regulatory and quantitative resource estimation, optimized ML

models offer flexibility, automation, and adaptability to nonlinear patterns that traditional geostatistics may fail to capture.

4.1. Limitations and future work

Despite the promising results, this study presents several limitations primarily related to data availability and spatial sampling density. The number of drillholes and sampling points, although adequate for an exploratory-scale study, may constrain the representativeness of the spatial model. Additionally, the analysis was restricted to a single deterministic interpolation technique (OK) without incorporating stochastic simulation methods such as Sequential Gaussian Simulation (SGS), which could better quantify spatial uncertainty. Future research should therefore include (i) denser sampling grids and the integration of new drillholes, (ii) the application of SGS and other conditional simulation techniques for uncertainty quantification, (iii) comparative analyses of advanced ensemble and deep learning models (StackingC, CNNs, or hybrid fractal-wavelet frameworks), and (iv) comprehensive techno-economic evaluations linking predicted grades to reprocessing feasibility and environmental impact.

This study provides a robust and reproducible methodological foundation for assessing the economic potential of gold tailings through the combined use of geostatistics and metaheuristic-optimized machine learning. The proposed framework can be extended to other abandoned deposits in Peru and similar geological environments worldwide, contributing to the sustainable revalorization of mine waste under the principles of circular mining.

References

[1]. Hudson-Edwards, K. A., Jamieson, H. E., & Lottermoser, B. G. (2011). Mine wastes: past, present, future. *Elements*, *7*(6), 375-380.

[2]. Abbadi, A., & Mucsi, G. (2024). A review on complex utilization of mine tailings: recovery of rare earth elements and residue valorization. *Journal of Environmental Chemical Engineering*, *12*(3), 1-18.

[3]. Edraki, M., Baumgartl, T., Manlapig, E., Bradshaw, D., Franks, D. M., & Moran, C. J. (2014). Designing mine tailings for better environmental, social and economic outcomes: a review of alternative approaches. *Journal of Cleaner Production*, *84*, 411-420.

[4]. Falagán, C., Grail, B. M., & Johnson, D. B. (2017). New approaches for extracting and recovering metals from mine tailings. *Minerals Engineering*, 106, 71-78.

[5]. Farhadi, S., Afzal, P., Konari, M. B., Saein, L. D., & Sadeghi, B. (2022). Combination of machine learning algorithms with concentration–area fractal method for soil geochemical anomaly detection in sediment-hosted Irankuh Pb–Zn deposit, central Iran. *Minerals*, *12*(6), 689.

[6]. Cotrina-Teatino, M. A., Marquina-Araujo, J. J., Mamani-Quispe, J. N., Chira-Fernandez, J. E., Castillo-Chung, A. R., Arango-Retamozo, S. M., González-Vasquez, J. A., & Ortiz-Quintanilla, S. M. (2025). Geochemical and mineralogical characterization of critical elements in gold tailings from the La Cienega, Peru, and assessment of their reuse potential. *Journal of Environmental Chemical Engineering*, *13*(5), 118497.

[7]. Lemos, M., Valente, T., Marinho Reis, P., Fonseca, R., Delbem, I., Ventura, J., & Magalhães, M. (2021). Mineralogical and geochemical characterization of gold mining tailings and their potential to generate acid mine drainage (Minas Gerais, Brazil). *Minerals, 11*(1), 39.

[8]. Lottermoser, B. (2010). Mine wastes Characterization, Treatment and Environmental Impacts. *Earth and Environmental Science*.

[9]. Lemos, M. G., Valente, T., Marinho-Reis, A. P., Fonsceca, R., Dumont, J. M., Ferreira, G. M. M., & Delbem, I. D. (2021). Geoenvironmental study of gold mining tailings in a circular economy context: Santa Barbara, Minas Gerais, Brazil. *Mine Water and the Environment*, 40, 257-269.

[10]. Parviainen, A., Kauppila, T., & Loukola-Ruskeeniemi, K. (2012). Long-term lake sediment records and factors affecting the evolution of metal(loid) drainage from two mine sites (SW Finland). *Journal of Geochemical Exploration, 114*, 46-56.

[11]. González-Díaz, E., García, S., Soto, F., Navarro, F., Townley, B., & Caraballo, M. A. (2022). Geochemical, mineralogical and geostatistical modelling of an IOCG tailings deposit (El Buitre, Chile): implications for environmental safety and economic potential. *Journal of Geochemical Exploration, 239*, 106997.

[12]. Kossoff, D., Dubbin, W. E., Alfredsson, M., Edwards, S. J., Macklin, M. G., & Hudson-Edwards, K. A. (2014). Mine tailings dams: characteristics, failure, environmental impacts, and remediation. *Applied Geochemistry, 51*, 229-245.

[13]. Lyu, Z., Chai, J., Xu, Z., Qin, Y., & Cao, J. (2019). A comprehensive review on reasons for tailings dam failures based on case history. *Advances in Civil Engineering, 2019*(1), 1-18.

[14]. Yin, Z., Sun, W., Hu, Y., Zhang, C., Guan, Q., & Wu, K. (2018). Evaluation of the possibility of copper recovery from tailings by flotation through bench-scale, commissioning, and industrial tests. *Journal of Cleaner Production, 171*, 1039-1048.

[15]. Araya, N., Ramírez, Y., Cisternas, L. A., & Kraslawski, A. (2021). Use of real options to enhance water–energy nexus in mine tailings management. *Appl Energy, 303*, 117626.

[16]. Cotrina-Teatino, M. A., & Marquina-Araujo, J. J. (2025). Circular economy in the mining industry: a

bibliometric and systematic literature review. *Resources Policy, 102*, 105513.

[17]. Shaforostova, E. N., Kosareva-Volod'ko, O. V., Belyankina, O. V., Solovykh, D. Y., Sazankova, E. S., Sizova, E. I., & Adigamov, D. A. (2023). A tailing dump as industrial deposit: study of the mineralogical composition of tailing dump of the Southern Urals and the possibility of tailings re-development. *Resources, 12*(2), 28.

[18]. Manaviparast, H. R., Miranda, T., Pereira, E., & Cristelo, N. (2024). A comprehensive review on mine tailings as a raw material in the alkali activation process. *Applied Sciences, 14*(12), 5127.

[19]. Pizarro Barraza, F., Thiyagarajan, D., Ramadoss, A., Manikandan, V. S., Dhanabalan, S. S., Abarzúa, C. V., Sotomayor Soloaga, P., Campos Nazer, J., Morel, M. J., & Thirumurugan, A. (2024). Unlocking the potential: mining tailings as a source of sustainable nanomaterials. *Renewable and Sustainable Energy Reviews, 202*, 114665.

[20]. Kinnunen, P., Ismailov, A., Solismaa, S., Sreenivasan, H., Räisänen, M. L., Levänen, E., & Illikainen, M. (2018). Recycling mine tailings in chemically bonded ceramics: a review. *Journal of Cleaner Production, 174*, 634-649.

[21]. Solismaa, S., Ismailov, A., Karhu, M., Sreenivasan, H., Lehtonen, M., Kinnunen, P., Illikainen, M., & Räisänen, M. L. (2018). Valorization of Finnish mining tailings for use in the ceramics industry. *Bulletin of the Geological Society of Finland, 90*, 33-54.

[22]. Spooren, J., Binnemans, K., Björkmalm, J., et al. (2020). Near-zero-waste processing of low-grade, complex primary ores and secondary raw materials in Europe: technology development trends. *Resources, Conservation and Recycling, 160*, 104919.

[23]. Vitti, C., & Arnold, B. J. (2022). The reprocessing and revalorization of critical minerals in mine tailings. *Mining, Metallurgy & Exploration, 39*, 49-54.

[24]. Cotrina-Teatino, M. A., Marquina-Araujo, J. J., Avalos-Murga, J. A., & Carrion-Villacorta, F. L. (2025). Flotation of mine tailings: a bibliometric analysis and systematic literature review. *Journal of Environmental Chemical Engineering, 13*(2), 116136.

[25]. Blannin, R., Frenzel, M., Tolosana-Delgado, R., Büttner, P., & Gutzmer, J. (2023). 3D geostatistical modelling of a tailings storage facility: resource potential and environmental implications. *Ore Geology Reviews, 154*, 105337.

[26]. Leskelä, T., Hokka, J., & Karlsson, T. (2025). Geostatistical modelling of mine tailings and comparative analysis of sampling methodologies: a case study of the Otanmäki ilmenite tailings storage facility project. *Journal of Geochemical Exploration, 274*, 107759.

[27]. Expósito-Suárez, V. M., Suárez-Navarro, J. A., Caro, A., et al. (2024). Radiological characterization of the tailings of an abandoned copper mine using a neural network and geostatistical analysis through the co-kriging method. *Environmental Geochemistry and Health, 46,* 297.

[28]. Parviainen, A., Soto, F., & Caraballo, M. A. (2020). Revalorization of Haveri Au–Cu mine tailings (SW Finland) for potential reprocessing. *Journal of Geochemical Exploration, 218*, 106614.

[29]. Soto, F., Navarro, F., Díaz, G., Emery, X., Parviainen, A., & Egaña, Á. (2022). Transitive kriging for modeling tailings deposits: a case study in southwest Finland. *Journal of Cleaner Production, 374*, 133857.

[30]. Cotrina-Teatino, M. A., & Marquina-Araujo, J. J. (2025). Geostatistical models, recovery, revalorization and economic potential in mine tailings: a comprehensive bibliometric and systematic review. *Journal of Cleaner Production, 509*, 145617

[31]. Madani, N., Maleki, M., & Parviainen, A. (2025). Enhancing multivariate geostatistical simulation in mine tailings using the projection pursuit multivariate transform and coregionalization analysis. *Mathematical Geosciences*.

[32]. García, S., Camus, L., Gonzalez-Diaz, E., Collao, R., Townley, B., Parviainen, A., & Caraballo, M. A. (2024). The importance of geochemical and mineralogical characterization of fresh Cu-porphyry mine tailings in mineral processing plants to optimize their revalorization potential. *Journal of Geochemical Exploration, 259*, 107439.

[33]. Nascimento, S. C., Cooke, D. R., Cracknell, M. J., Miller, C. B., & Parbhakar-Fox, A. (2025). Mineralogical and geochemical characterization of mine tailings in the King River Delta, Western Tasmania: implications for long-term stability of trace elements. *Applied Geochemistry, 184*, 106366

[34]. Redwan, M., & Bamousa, A. O. (2019). Characterization and environmental impact assessment of gold mine tailings in arid regions: a case study of Barramiya gold mine area, Eastern Desert, Egypt. *Journal of African Earth Sciences, 160*, 103644.

[35]. Samanta, B., Bandopadhyay, S., & Ganguli, R. (2002). Data segmentation and genetic algorithms for sparse data division in Nome placer gold grade estimation using neural network and geostatistics. *Exploration and Mining Geology, 11*(1–4), 69–76

[36]. Kaplan, U. E., & Topal, E. (2020). A new ore grade estimation using combine machine learning algorithms. *Minerals*, 10(10), 847.

[37]. Marquina-Araujo, J. J., Cotrina-Teatino, M. A., Mamani-Quispe, J. N., Noriega-Vidal, E. M., Vega-Gonzalez, J. A., & Cruz-Galvez, J. (2024). Copper ore grade prediction using machine learning techniques in a copper deposit. *Journal of Mining and Environment, 15*(3), 1011–1027.

[38]. Maniteja, M., Samanta, G., Gebretsadik, A., Tsae, N. B., Rai, S. S., Fissha, Y., Okada, N., & Kawamura, Y. (2025). Advancing iron ore grade estimation: a comparative study of machine learning and ordinary kriging. *Minerals, 15*(2), 131.

[39]. Dey, T., & Samanta, G. (2025). Grade estimation using machine learning techniques in Indian copper deposits. *Journal of The Institution of Engineers (India): Series D, 106*(1), 717–723

[40]. Tsae, N. B., Adachi, T., & Kawamura, Y. (2023). Application of artificial neural network for the prediction of copper ore grade. *Minerals, 13*(5), 658.

[41]. Bazdar, H., Fattahi, H., & Ghadimi, F. (2015). Hybrid ANN with invasive weed optimization algorithm, a new technique for prediction of gold and silver in Zarshuran gold deposit, Iran. *Journal of Tethys, 3*(3), 273–285

[42]. Yu, S., Zhu, K., & He, Y. (2012). A hybrid intelligent optimization method for multiple metal grades optimization. *Neural Computing and Applications, 21*(6), 1391–1402

[43]. Jafrasteh, B., Fathianpour, N., & Suárez, A. (2018). Comparison of machine learning methods for copper ore grade estimation. *Computational Geosciences, 22*, 1371–1388.

[44]. Farhadi, S., Tatullo, S., Boveiri Konari, M., & Afzal, P. (2024). Evaluating StackingC and ensemble models for enhanced lithological classification in geological mapping. *Journal of Geochemical Exploration, 260*, 107441

[45]. Zhao, J., Chi, H., Shao, Y., & Peng, X. (2022). Application of AdaBoost algorithms in Fe mineral prospectivity prediction: a case study in Hongyuntan–Chilongfeng mineral district, Xinjiang Province, China. *Natural Resources Research, 31*, 2001–2022.

[46]. Li, T., Xia, Q., Ouyang, Y., Zeng, R., Liu, Q., & Li, T. (2024). Prospectivity and uncertainty analysis of tungsten polymetallogenic mineral resources in the Nanling metallogenic belt, South China: a comparative study of AdaBoost, GBDT, and XGBoost algorithms. *Natural Resources Research, 33*, 1049–1071.

[47]. Pourgholam, M. M., Adib, A., Afzal, P., Rahbar, K., & Gholinejad, M. (2025). Deep learning and fractal-wavelet techniques for magnetite-apatite exploration in Tarom, Iran. *Scientific Reports, 15*(1), 31907.

[48]. Cotrina-Teatino, M. A., Marquina-Araujo, J. J., Mamani-Quispe, J. N., Guartán, J. A., Castillo-Chung, A. R., Arango-Retamozo, S. M., González-Vasquez, J. A., & Ortiz-Quintanilla, S. M. (2025). Strategic potential assessment of lanthanum and scandium through geochemical–lithological analysis with unsupervised machine learning in southern Ecuador. *Resources Policy, 109*, 105731.

[49]. Manrique, M., & Agurto, A. (2022). Caracterización geoquímica y mineralógica de relaves mineros La Ciénaga – La Libertad. *INGEMMET, Boletín, Serie B: Geología Económica, 78*, 143.

[50]. Walsh Perú. (2017). El Entorno Social: Estudio de caso de pasivos ambientales mineros en la región La Libertad / Perú. Las Relaveras de La Ciénaga / Pataz. Santiago: Cooperación Alemana para el Desarrollo; Instituto Federal de Geociencias y Recursos Naturales (BGR).

[51]. Meyer, C., Jerez, I., & Soundy, R. (2019). Relaves "La Ciénaga" Pataz en Perú: Informe sobre caso de estudio para la remediación de los relaves en La Ciénaga, Pataz en Perú. *UMTEC – Biener / Sasse / Konertz – Partnerschaft Beratender Ingenieure und Geologen mbB, 47*.

[52]. Mpinga, C. N., Bradshaw, S. M., Akdogan, G., Snyders, C. A., & Eksteen, J. J. (2014). Evaluation of the Merrill–Crowe process for the simultaneous removal of platinum, palladium and gold from cyanide leach solutions. *Hydrometallurgy, 142*, 36–46.

[53]. Haeberlin, Y. (2002). Geological and structural setting, age, and geochemistry of the orogenic gold deposits at the Pataz Province, Eastern Andean Cordillera, Peru. *Terre et Environnement, 36*, 182.

[54]. Schreiber, D. W., Fontboté, L., & Lochmann, D. (1990). Geologic setting, paragenesis, and physicochemistry of gold quartz veins hosted by plutonic rocks in the Pataz region. *Economic Geology, 85*(7), 1328–1347.

[55]. Witt, W. K., Hagemann, S. G., Villanes, C., Vennemann, T., Zwingmann, H., Laukamp, C., & Spangenberg, J. E. (2016). Multiple gold mineralizing styles in the Northern Pataz District, Peru. *Economic Geology, 111*(2), 355–394.

[56]. Mendoza, A. (2016). Estudio de potencial neto de neutralización de dos muestras de relaves. Informe técnico, abril 2016. Investigación Metalúrgica No. 18148, BGR Chile.

[57]. Morche, W. (2017). Estudio de caso de pasivos ambientales mineros en la región La Libertad/Perú: Las relaveras de La Ciénaga/Pataz. Investigación económico-minera y ambiental. Cooperación Alemana para el Desarrollo – Instituto Federal de Geociencias y Recursos Naturales (BGR), Trujillo (Perú) – Santiago (Chile).

[58]. Oré, G. (2017). Gisement de Poderosa (Pérou): une minéralisation aurifère filonienne de filiation magmatique. Thèse de doctorat, Université du Québec à Chicoutimi, Québec, Canada.

[59]. Voute, F., Hagemann, S. G., Evans, N. J., & Villanes, C. (2019). Sulfur isotopes, trace element, and textural analyses of pyrite, arsenopyrite and base metal sulfides associated with gold mineralization in the Pataz-Parcoy district, Peru: Implication for paragenesis, fluid source, and gold deposition mechanisms. *Mineralium Deposita, 54*(7), 1077–1100.

[60]. Pesquer, L., Cortés, A., & Pons, X. (2011). Parallel ordinary kriging interpolation incorporating automatic variogram fitting. *Computers & Geosciences, 37*(4), 464–473.

[61]. Ramadhan, M. D., Marwanza, I., Nas, C., Azizi, M. A., Dahani, W., & Kurniawati, R. (2021). Drill holes spacing analysis for estimation and classification of coal resources based on variogram and kriging. *IOP Conference Series: Earth and Environmental Science*, 819, 012026.

[62]. Deutsch, C. V. (1996). Correcting for negative weights in ordinary kriging. *Computers & Geosciences, 22*(7), 765–773.

[63]. Wackernagel, H. (2003). Ordinary kriging. In Multivariate geostatistics: An introduction with applications (3rd ed., pp. 79–88). Springer, Berlin, Heidelberg.

[64]. Cotrina-Teatino, M. A., Marquina-Araujo, J. J., & Riquelme, Á. I. (2025). Comparison of machine learning techniques for mineral resource categorization in a copper deposit in Peru. *Natural Resources Research, 34*(4), 2007–2025.

[65]. Xiong, J., Gong, Y., Liu, X., Li, Y., Chen, L., Liao, C., & Zhang, C. (2025). A PSO-XGBoost model for predicting the compressive strength of cement–soil mixing pile considering field environment simulation. *Buildings, 15*(15), 2740.

[66]. Gu, Y., Zhang, D., & Bao, Z. (2021). A new data-driven predictor, PSO-XGBoost, used for permeability of tight sandstone reservoirs: A case study of member of Chang 4+5, western Jiyuan Oilfield, Ordos Basin. *Journal of Petroleum Science and Engineering, 199*, 108350.

[67]. Ngoc, L. T., Nguyen, H., Bui, X.-N., & Tran, T.-T. (2025). Dynamic weighting and genetic algorithm-based hybrid SVR–Ridge model for improving PM2.5 forecasting in open-pit copper mines. *International Journal of Mining, Reclamation and Environment*, 1–31.

[68]. Zhang, J., Xu, L., Li, J., Yan, Y., & Xu, R. (2022). Parameter acquisition study of mining-induced surface subsidence probability integral method based on RF–AGA–ENN model. *Geofluids, 2022*, 1865004.

[69]. Parsa, M. (2021). A data augmentation approach to XGBoost-based mineral potential mapping: An example of carbonate-hosted Zn–Pb mineral systems of western Iran. *Journal of Geochemical Exploration, 228*, 106811.

[70]. Nabavi, Z., Mirzehi, M., Dehghani, H., & Ashtari, P. (2023). A hybrid model for back-break prediction using XGBoost machine learning and metaheuristic algorithms in Chadormalu iron mine. *Journal of Mining and Environment, 14*(2), 689–712.

[71]. Li, T., Xia, Q., Ouyang, Y., Zeng, R., Liu, Q., & Li, T. (2024). Prospectivity and uncertainty analysis of tungsten polymetallogenic mineral resources in the Nanling metallogenic belt, South China: A comparative study of AdaBoost, GBDT, and XgBoost algorithms. *Natural Resources Research, 33*(4), 1049–1071.

[72]. Cotrina, M., Marquina, J., & Polo, J. (2025). Prediction of unit haulage cost in an underground mine using machine learning techniques. *Journal of Sustainable Mining, 24*(2), 250–266.

[73]. Hasanipanah, M., Amnieh, H. B., Arab, H., & Zamzam, M. S. (2018). Feasibility of PSO–ANFIS model to estimate rock fragmentation produced by mine blasting. *Neural Computing and Applications, 30*(4), 1015–1024.

[74]. Liu, W., & Zhang, H. (2016). PSO algorithm for block sequencing problem in open pit mining. *In Proceedings of the 2015 5th International Conference on Computer Sciences and Automation Engineering,* 434–441.

[75]. Goswami, A. D., Mishra, M. K., & Patra, D. (2022). Evaluation of machine learning algorithms for grade estimation using GRNN & SVR. *Engineering Research Express, 4*(3), 035037.

[76]. Cotrina, M., Marquina, J., Mamani, J., Arango, S., Gonzalez, J., Ccatamayo, J., & Noriega, E. (2025). Hybrid machine learning techniques to predict fuel consumption of dump trucks in an open-pit mine in Peru. *International Journal of Mining and Mineral Engineering, 16*(1), 1–20.

[77]. Breiman, L. (2001). Random forests. *Machine Learning, 45*(1), 5–32.

[78]. Acorn, T., Boisvert, J. B., & Leuangthong, O. (2020). Managing geologic uncertainty in pit shell optimization using a heuristic algorithm and stochastic dominance. *Mining, Metallurgy & Exploration, 37*(2), 375–386.

[79]. Cristianini, N. (2004). Cross-validation (K-fold cross-validation, leave-one-out, jackknife, bootstrap). *In Dictionary of Bioinformatics and Computational Biology*. John Wiley & Sons.

[80]. Bayat, P., Monjezi, M., Rezakhah, M., & Armaghani, D. J. (2020). Artificial neural network and firefly algorithm for estimation and minimization of ground vibration induced by blasting in a mine. *Natural Resources Research, 29*(6), 4121–4132.

[81]. Cotrina, M., Marquina, J., Mamani, J., Ccatamayo, J., Gonzalez, J., Arango, S., & Noriega, E. (2024). Predictive model using machine learning to determine fuel consumption in CAT-777F mining equipment. *International Journal of Mining and Mineral Engineering, 15*(2), 147–160.

[82]. Cotrina, M., Marquina, J., Noriega, E., Mamani, J., Ccatamayo, J., Gonzalez, J., & Arango, S. (2024). Predicting open pit mine production using machine learning techniques: A case study in Peru. *Journal of Mining and Environment, 15*(4), 1345–1355.

انجمن مهندسی معدن ایران
نشریه مهندسی معدن و محیط زیست
نشانی نشریه: www.jme.shahroodut.ac.ir
دانشگاه صنعتی شاهرود

ارزش گذاری مجدد باطله‌ها در La Cienega (پرو) از طریق مدل‌سازی ژئوشیمیایی، زمین آماری و یادگیری ماشینی بهینه شده توسط فراابتکاری

مارکو آنتونیو کوترینا-تاتینو[۱*]، ژایرو جاناتان مارکینا-آراوخو[۱]، خوزه نستور مامانی-کوئیسپه[۲]، خورخه چیرا-فرناندز[۳]، سزار دلا کروز-پوما[۳]، و سولیو مارینو آرانگو-رتاموزو[۱]

۱. گروه مهندسی معدن، دانشکده مهندسی، دانشگاه ملی تروخیلو، تروخیلو، پرو
۲. دانشکده مهندسی شیمی، دانشگاه ملی آلتیپلانو پونو، پونو، پرو
۳. اداره منابع معدنی و انرژی، INGEMMET، لیما، پرو

اطلاعات مقاله

تاریخ ارسال: ۲۰۲۵/۰۷/۰۳
تاریخ داوری: ۲۰۲۵/۱۰/۰۷
تاریخ پذیرش: ۲۰۲۵/۱۲/۰۹

DOI: 10.22044/jme.2025.16468.3212

کلمات کلیدی

باطله‌های معدن
بازفرآوری زباله
زمین‌آمار
یادگیری ماشین
متاهیوریستیک

چکیده

افزایش مداوم ضایعات معدنی، به ویژه به شکل باطله‌ها، یک چالش زیست‌محیطی و اقتصادی قابل توجه ایجاد می‌کند، به خصوص در زمینه‌هایی که این ذخایر حاوی محتوای فلزی باقیمانده هستند. این مطالعه پتانسیل طلای سپرده باطله I در لا سینگا (پرو) را با ادغام مدل‌های تخمین زمین‌آماری و یادگیری ماشینی بهینه شده از طریق الگوریتم‌های فراابتکاری ارزیابی کرد. این روش شامل توصیف ژئوشیمیایی، تخمین سه‌بعدی با استفاده از کریجینگ معمولی (OK) به عنوان یک روش زمین‌آماری و پیش‌بینی عیارهای طلا از طریق سه مدل بود: XGBoost بهینه شده با بهینه‌سازی ازدحام ذرات (XGB+PSO)، رگرسیون بردار پشتیبان با الگوریتم ژنتیک (SVR+GA) و جنگل تصادفی بهینه شده با استفاده از بهینه‌سازی کلونی مورچه‌ها (RF+ACO). تخمین‌ها با استفاده از اعتبارسنجی متقابل Leave-One-Out و معیارهای عملکرد شامل RMSE، MAE، بایاس و ضریب همبستگی (R) اعتبارسنجی شدند. مدل RF+ACO به RMSE برابر با ۰.۳۲ ppm، MAE برابر با ۰.۲۴ ppm، Bias برابر با ۰.۰۰۶ و مقدار R برابر با ۰.۵۶ دست یافت. میانگین عیارهای پیش‌بینی‌شده از ۱.۱۴ تا ۱.۳۳ ppm متغیر بود و میزان طلای تخمینی بین ۹۸۱.۰۰ تا ۱۱۴۷.۱۲ اونس بود، در حالی که OK 1028.77 اونس با عیار متوسط ۱.۱۹ ppm به دست آورد. این یافته‌ها نشان می‌دهد که مدل‌های یادگیری ماشینی که به درستی بهینه شده‌اند، می‌توانند تخمین‌های معقولی از میزان فلز در باطله‌ها، به‌ویژه در مناطقی که با ناهمگونی مکانی بالا و پیوستگی زمین‌شناسی محدود مشخص می‌شوند، ارائه دهند.

نویسنده مسئول مکاتبات: mcotrinat@unitru.edu.pe (م. الف. ک. تاتینو)